nature materials

REVIEW ARTICLE

PUBLISHED ONLINE: 23 JANUARY 2018 | DOI: 10.1038/NMAT5063

Organic solar cells based on non-fullerene acceptors

Jianhui Hou[1]*, Olle Inganäs[2], Richard H. Friend[3] and Feng Gao[2]*

Organic solar cells (OSCs) have been dominated by donor:acceptor blends based on fullerene acceptors for over two decades. This situation has changed recently, with non-fullerene (NF) OSCs developing very quickly. The power conversion efficiencies of NF OSCs have now reached a value of over 13%, which is higher than the best fullerene-based OSCs. NF acceptors show great tunability in absorption spectra and electron energy levels, providing a wide range of new opportunities. The coexistence of low voltage losses and high current generation indicates that new regimes of device physics and photophysics are reached in these systems. This Review highlights these opportunities made possible by NF acceptors, and also discuss the challenges facing the development of NF OSCs for practical applications.

Light absorption in organic semiconductors generates strongly bound excitons. Donor (D):acceptor (A) bulk-heterojunction (BHJ) structures, suitable for low-cost solution processing, provide an efficient approach to split the excitons into free carriers[1,2]. Among different acceptor materials, fullerene derivatives attracted the most attention and gave the highest power conversion efficiencies (PCEs) for almost two decades. Unique to fullerene derivatives is their ball-like fully conjugated structure, which provides strong electron-accepting and isotropic electron-transport capabilities and facilitates electron delocalization at the D:A interfaces[3]. As such, fullerene derivatives were believed to be a critical component for efficient operation of organic solar cells (OSCs). Indeed, acceptor materials based on molecules other than fullerene derivatives, generally categorized as non-fullerene (NF) acceptors, usually resulted in low PCEs[1,4], which were mainly attributed to the difficulties in the morphological control[5].

However, this situation has changed recently. The PCEs of NF OSCs have increased dramatically since 2015, now reaching a high value of 13.1% (ref. 6). At present, such a high value is better than the efficiency obtained in the best fullerene-based OSCs[7,8]. The quick development of NF OSCs during the past two years has benefited a lot from the synthetic methods, materials design strategies and device engineering protocols developed during the past two decades for fullerene-based OSCs. The wide range of donor molecules developed for fullerene-based OSCs provides a rich library for immediate use in NF OSCs. In addition, various design strategies originally developed for donor molecules are readily available to tune the absorption spectra and energy levels of NF acceptors, allowing better flexibility in realizing donor-acceptor systems with complementary absorption and optimized energy band diagram. The development of a few high-performing molecules, discussed in the next section, has also contributed to attracting the interest of the research community on NF OSCs.

From the device point of view, the fact that excitons can separate efficiently upon negligible driving energies[9–14] contributes to high PCEs in NF OSCs. As a result, NF OSCs often show high photocurrent and low voltage losses at the same time. In contrast, charge separation in fullerene-based OSCs usually becomes problematic under low driving energies, presenting a trade-off between high photocurrent and high photovoltage[15,16]. Currently, the device physics and photophysics investigations are lagging behind the rapid developments of materials and device engineering. A fundamental question open to the community is how the excitons split into free carriers in these NF OSCs with low driving energies.

One of the key challenges for NF acceptors might lie in their anisotropic structures. It is well acknowledged that D:A π–π interactions, which depend on the molecular orientation between the donor and acceptor materials, are very important for the charge transfer and transport in the devices[17]. Compared with the isotropic ball-like conjugated backbones in fullerene derivatives, the anisotropic conjugated structures of NF acceptors make it more challenging to ensure efficient π–π interactions[18–21]. Therefore, in NF OSCs, it becomes critically important to pair the donors with acceptors that have the right chemical structure, which must ensure optimal molecular orientation as well as fine-tuned phase separation.

The development of NF acceptors presents opportunities that are otherwise not possible in fullerene-based OSCs, and also opens up challenges that are waiting to be tackled for future applications of this promising technology. In addition, the operation of NF OSCs also implies new working mechanisms, which could be fundamentally different from those in fullerene-based OSCs. This Review aims to discuss these opportunities, challenges and working mechanisms, hoping to foster further advances in this field. The PCEs of NF OSCs are likely to be further improced, through both materials chemistry and device engineering. As such, NF OSCs provide a promising technology for practical applications in the near future, especially considering that they have also shown excellent thermal stability[22,23].

State-of-the-art non-fullerene acceptors

Based on chemical structures, state-of-the-art NF acceptors can be categorized into two types: acceptors based on fused aromatic diimides, and acceptors based on strong intramolecular electron push–pulling effects. These high-performance NF acceptors share two features in common (Fig. 1a). First, their conjugated backbones are modified with π-conjugated functional groups involving highly electronegative elements—for example, oxygen (in the form of a carbonyl group) and/or nitrogen (in the forms of a cyano group or nitrogen-containing hetero-aromatic segments). Second, π-electrons in these functional groups can be well delocalized into the backbones. The first feature provides strong electron-accepting

[1]Beijing National Laboratory for Molecular Sciences, State Key Laboratory of Polymer Physics and Chemistry, Institute of Chemistry, Chinese Academy of Sciences, Beijing 100190, China. [2]Biomolecular and organic electronics, Department of Physics, Chemistry and Biology (IFM), Linköping University, Linköping SE-58183, Sweden. [3]Cavendish Laboratory, J J Thomson Avenue, Cambridge CB3 0HE, UK. *e-mail: hjhzlz@iccas.ac.cn; fenga@ifm.liu.se

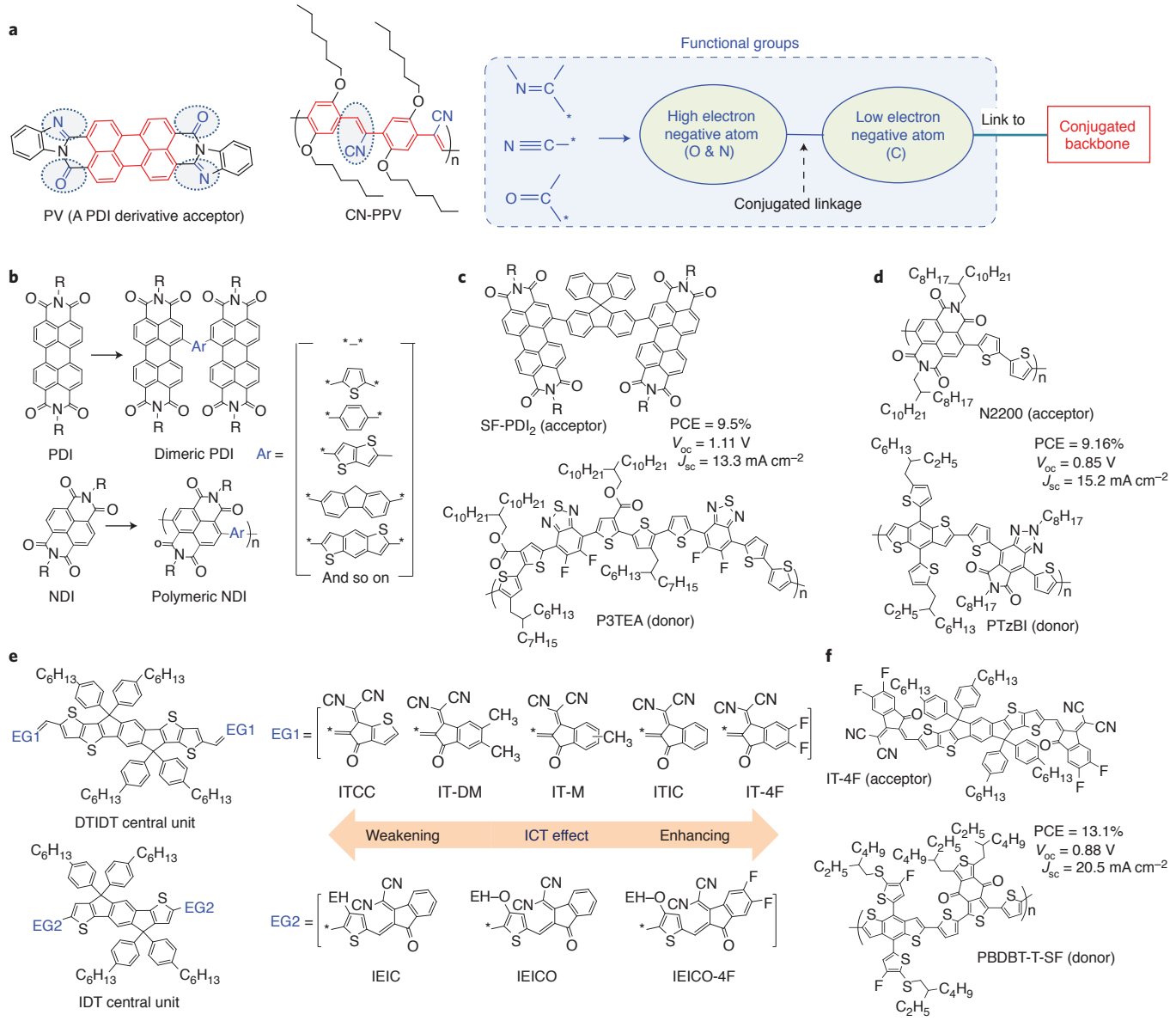

Figure 1 | State-of-the-art NF acceptors. a, Key features of successful NF acceptors (PV and CN-PPV are the first NF acceptor materials used in the heterojunction and bulk heterojunction OSCs, respectively): the functional groups, which are linked by high electron negative atoms (for example, oxygen or nitrogen) and low electron negative atoms (usually carbon) through a conjugated linkage, offer strong electron accepting capabilities. These functional groups are then linked to conjugated backbones. **b**, Two typical types of acceptor materials based on aromatic diimide derivatives: dimeric PDIs and polymeric NDIs, where Ar represents the linkers between the units. **c**, Performance and molecular structures of NF OSCs using small-molecule aromatic diimides (SF-PDI_2) as the acceptor and P3TEA as the donor. **d**, Performance and molecular structures of NF OSCs using polymeric aromatic diimides (N2200) as the acceptor and PTzBI as the donor. **e**,**f**, Molecular structures of eight ITIC-like acceptors with different intramolecular charge transfer (ICT) effects, with the structures and photovoltaic performance of the combination PBDBT-T-SF: IT-4F shown in **f**.

abilities, and the second feature ensures a relatively low reorganization energy so that the accepted electrons can be transported easily without being trapped. In addition, for solution-processed OSCs, appropriate functional groups also need to be carefully designed to satisfy the solubility requirement—this is different to vacuum-deposited OSCs. We note that in vacuum-deposited solar cells, NF acceptors also demonstrate great potential in enhancing light absorption and hence attract considerable attention[24,25], consistent with recent development in solution-processed OSCs.

Acceptors based on fused aromatic diimides. Fused aromatic diimide derivative was the first acceptor material used in heterojunction OSCs—it was used as the electron acceptor in the pioneering bilayer devices in 1986 (Fig. 1a)[26]. Since then, this type of material has been considered as a promising candidate for NF OSCs. Among various derivatives of fused aromatic diimides, perylene diimides (PDIs) and naphthalene diimides (NDIs) (Fig. 1b), widely used in the traditional dye industry, are two of the most intensively studied acceptor molecules because of their advantages in strong light absorption, low synthesis cost and excellent stability.

PDIs have been frequently used in small molecular acceptors[27]. The key considerations for the molecular design of PDI-based acceptors are to restrain their aggregation effects and improve their miscibility with polymer donors. PDIs have rigid and planar conjugated

backbones. As a result, the PDI derivatives in solid state tend to form large-sized crystals, which are undesirable for the nanoscale morphology in the BHJ structures[4]. In addition to approaches of general applicability (for instance, side chain engineering and solvent engineering) for controlling aggregation effects, an effective method to solving this problem is to link PDI units, forming dimeric or multilinked PDIs (Fig. 1b)[28–30]. These linked PDI derivatives are twisted, helping to break the aggregation of PDIs. For example, an efficient OSC based on a PDI derivative was obtained by using a dimer named as SF-PDI$_2$, where two *N*-alkyl-substituted PDIs were linked by an unsubstituted spirofluorene (Fig. 1c)[9].

In addition to small molecules, polymers based on fused aromatic diimides (for instance, *N*-alkyl-substituted PDIs and NDIs) have also been employed as effective acceptors in all-polymer OSCs[31–34]. The linkers also play a critical role in the design of these polymer acceptors. In this case, they not only help to modulate the aggregation but also provide additional opportunities to decrease the bandgap due to their extended conjugation. As a result, the polymer acceptors based on fused aromatic diimide derivatives often demonstrate low bandgaps. For example, N2200 (Fig. 1d), which is a popular polymer acceptor based on NDI and bithiophene, has a low bandgap of 1.46 eV. Its absorption spectrum and energy levels match very well with a range of wide and mid bandgap polymer donors originally developed for fullerene-based OSCs. Up to now, high PCEs around 9% have been obtained for all-polymer OSCs based on N2200[34,35].

In spite of this progress, the application of fused aromatic diimide-based polymer acceptors in OSCs present critical issues to be tackled. For example, there is a delicate balance between good solubility and effective interchain π–π interactions for PDI-based polymer acceptors. Highly twisting linkers help to provide good solubility, but prevent effective interchain π–π interactions, unfavourable for intermolecular charge transfer and transport. As a result, the linkers with decreased twisting effects are often used in these polymeric acceptors. In this case, long and branched alkyls, which offer sufficient solvation, have to be employed as the functional groups in order to ensure good solubility. However, these long branched alkyls are optoelectronically inert. This delicate requirement limits the development of suitable polymer acceptors. N2200 makes a good balance between high solubility and strong π–π interactions, and hence it has become the most widely used polymeric acceptor in NF OSCs. Another challenge intrinsic to the formation of BHJ structures through the mixing of polymeric donors and acceptors is to minimize phase separation while avoiding interchain entanglement between the different polymers. As subtle changes in chemical structures could significantly affect the delicate balance and hence the device performance, systematic investigations on the molecular structures have to be carried out to further improve the performance of all-polymer OSCs.

Acceptors based on strong intramolecular electron push–pulling effects. The first acceptor in this category, CN-PPV (Fig. 1a), was reported in a pioneering work on BHJ OSCs[1]. As the cyano group has high electron negativity and is linked with the ethylene segment, accepted electrons can delocalize effectively along the conjugated backbone of CN-PPV. Although the efficiency of OSCs based on CN-PPV acceptor is low (efficiencies up to 2%; see ref. 36), the development of this material triggered efforts in synthesizing polymeric or small-molecular acceptors based on functional groups with strong electron negativity.

In 2015, a high-performing material, with the abbreviated name of ITIC (structure shown in Fig. 1e), was developed following these guidelines[37]. Since then, the best photovoltaic performance for NF OSCs have been obtained with ITIC derivatives (Fig. 1f)[6,22,38]. The molecular energy levels and absorption spectra of ITIC derivatives can be effectively tuned by manipulating the intramolecular electron push–pulling effects while keeping their key features as efficient acceptor materials (Fig. 2a,b). Easy tunability makes great contributions to the rapid progress in PCEs for NF OSCs. For example, as shown in Fig. 2b, the lowest unoccupied molecular orbital (LUMO) level can be increased by incorporating electron-rich groups like methyl or methoxy into the end-capping units of ITIC, resulting in a molecule called IT-M. Using the same donor polymer, the IT-M-based device has a higher open-circuit voltage (V_{OC}) value than the ITIC-based device (resulting in an enhanced PCE of 12.1% as reported in ref. 38). At the same time, the LUMO level of ITIC could also be reduced by incorporating electron-deficient elements like F-atoms into the end-capping groups, resulting in a molecule called IT-4F. Since the electron-pulling effect of the end groups and hence the intramolecular charge transfer (ICT) effects are enhanced in IT-4F, this molecule shows a low LUMO level, red-shifted absorption and strong extinction coefficient. In order to make good use of the broad and strong light absorption capability of IT-4F without sacrificing the V_{OC}, a polymer named PBDB-T-SF (shown in Fig. 1f) with a low LUMO level was employed as the donor material. As a result, the device based on PBDB-T-SF:IT-4F gave a high efficiency of 13.1% with a short-circuit current (J_{SC}) of 20.5 mA cm^{-2} (ref. 6).

A critical question to the OSC materials community is: what makes ITIC derivatives so unique, in addition to their low bandgap and strong electron accepting capability? We believe that the key might lie in the favourable π–π interactions enabled by the molecular geometry (Fig. 2c–e). In ITIC derivatives, it is the electron-deficient end-capping units that form π–π interactions with the polymer donors and/or the adjacent acceptor molecules in blend film, facilitating efficient electron transfer and transport. Instead, the electron-rich central unit is not involved in π–π interactions due to the steric hindrance of the non-conjugated side groups[39]. We notice that this feature is also applicable to other high-efficiency acceptors based on strong intramolecular electron push–pulling effects. For example, a small molecular acceptor, namely EH-IDTBR[40], though different from ITIC derivatives in chemical structures, also has electron-deficient end-capping units for π–π interactions and an electron-rich core whose π orbitals are shielded by non-conjugated side groups.

Efficient charge separation upon small driving energies

Compared with fullerene-based OSCs, the most striking feature of NF-based OSCs is that a wide range of devices show efficient charge generation upon small (even negligible) driving energies[9–14]. Driving energy, traditionally believed to be necessary to split the strongly bound excitons at the D:A interfaces, constitutes an additional voltage loss for OSCs[41–43]. Previous investigations on fullerene-based OSCs revealed that charge generation could be efficient when the driving energy is decreased to a certain threshold, below which charge generation usually decreases dramatically[15,16]—although one exception was also reported[44]. Therefore, there is usually a trade-off between high photocurrent and small voltage loss for fullerene-based OSCs, limiting the power conversion efficiency. Instead, for NF OSCs, it has been demonstrated that the internal quantum efficiency can approach 90% even when the driving energy approaches zero—for instance, in the P3TEA:SF-PDI$_2$ blend[9]. This is the reason why a range of NF OSCs show high J_{SC} and large V_{OC} at the same time[10–14,45]. At this stage, it is not clear whether the tolerance with small driving energies comes from some special properties of the NF acceptors or merely from the fact that NF acceptors provide more opportunities to obtain aligned energetic levels between the donor and acceptor materials.

In the context of this Review, the driving energy is defined as the difference between the bandgap (E_{gap}) of the D:A materials (whichever has a smaller bandgap) and the energy of the charge-transfer

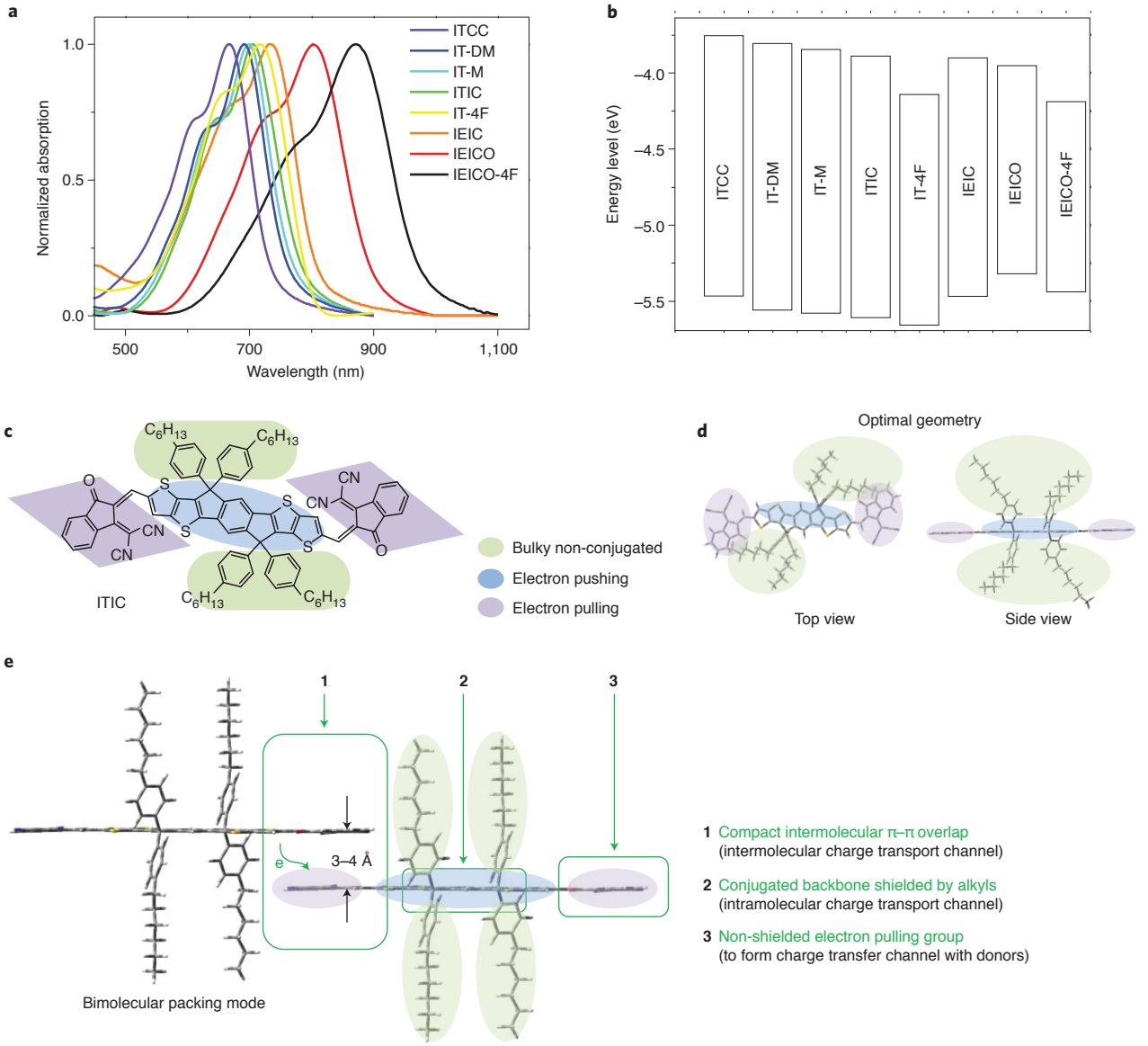

Figure 2 | Unique features of ITIC and its derivatives. a,**b**, The absorption spectra (**a**) and molecular energy levels (**b**) of the ITIC-like molecules in Fig. 1e can be easily tuned by modulating ICT effects. The molecular energy levels were estimated from the electrochemical cyclic voltammetry measurements. **c**, The ITIC molecule includes electron-pushing and electron-pulling units, where the electron-pushing units are shield by bulky non-conjugated side chains. **d**, Top and side views of the optimal geometry of the ITIC molecule. **e**, Bimolecular packing mode indicates that the electron-deficient end-capping units form π-π interactions with the adjacent acceptor molecule for efficient intermolecular charge transport and with the donor materials for efficient charge transfer. The electron-rich central unit is not involved in π-π interactions due to the steric hindrance of the non-conjugated side groups, and is only involved in intramolecular charge transport. Adapted from ref. 39, Wiley (**d**,**e**).

(CT) state when the electron–hole pair is still confined to the heterojunction, prior to long-range separation[3,15]. Although it is an important parameter, the E_{gap} in literature was usually arbitrarily determined from the absorption onset. An appropriate approach might be to use the crossing point between the normalized absorption and luminescence spectra to determine the E_{gap} (refs 9,46). This crossing point corresponds to the energy of the transition from the zeroth vibrational ground state to the zeroth vibrational first excited state. An alternative approach suggests the use of the inflection point of the external quantum efficiency (EQE) spectrum at long wavelengths to determine the E_{gap} (ref. 47). Given that EQE measurements are routinely reported in photovoltaic research articles, this method can be conveniently used to extract E_{gap} from this literature; moreover, it might be particularly advantageous for analysing materials whose absorption onset shifts upon mixing. The CT energies can be determined by measuring the absorption and/or emission from the CT states by using highly sensitive photothermal deflection spectroscopy, Fourier-transform photocurrent spectroscopy-EQE (FTPS-EQE) or electroluminescence (EL) measurements[48–50]. For systems with large driving energies, a redshift in the absorption and emission spectra of CT states will be observed compared with those of the singlet excitons from the pristine donor or acceptor materials[15]. In contrast, for systems with negligible driving energies, the absorption and emission of the devices will be dominated by those from the pristine donor or acceptor materials (Fig. 3a)[9,46].

Note that a small driving energy approaching zero does not necessarily guarantee a small voltage loss, as the voltage losses in OSCs include the contributions from both the loss due to charge transfer (that is, the driving energy) and the loss due to non-radiative

recombination. More specifically, the voltage losses can be categorized into three contributions (Fig. 3b)[9]:

$$\begin{aligned} q\Delta V &= E_{gap} - qV_{OC} \\ &= (E_{gap} - qV_{OC}^{SQ}) + (qV_{OC}^{SQ} - qV_{OC}^{rad}) \\ &\quad + (qV_{OC}^{rad} - qV_{OC}) \\ &= (E_{gap} - qV_{OC}^{SQ}) + q\Delta_{OC}^{rad,\,below\,gap} + qV_{OC}^{non-rad} \\ &= \Delta E_1 + \Delta E_2 + \Delta E_3 \end{aligned} \quad (1)$$

V_{OC}^{SQ} in the equation is the maximum voltage based on the Shockley–Queisser limit, where the EQE is assumed to be step-wise, that is, 1 above the gap and 0 below the gap[51]. Those who are interested in the details of different terms in equation (1) are referred to the supplementary information of ref. 9. The first term of energy loss in equation (1) ($E_{gap} - qV_{OC}^{SQ}$) is due to the mismatch between radiation received in a narrow solid angle from the sun and omnidirectional radiative recombination originating from the absorption above the bandgap. This loss is unavoidable for any type of solar cells and is typically 0.25 eV or above[52]. The second term in the equation ($qV_{OC}^{rad,below\,gap} = qV_{OC}^{SQ} - qV_{OC}^{rad}$) is due to additional radiative recombination from the absorption below the bandgap. For fullerene-based OSCs, the absorption from the CT states (that is, due to the existence of driving energy) is the main contribution of this term, which can be as large as 0.67 eV in the benchmark poly(3-hexylthiophene):[6,6]-phenyl-C_{61}-butyric acid methyl ester blend[52]. In the systems with negligible driving energies, CT state absorption becomes invisible, as the CT state energy is close to the singlet exciton energy. In this case, this term is only from the non-ideal absorption edge and can be decreased to 0.07 eV in the P3TEA:SF-PDI_2 blend[9]. The third loss term ($qV_{OC}^{non-rad} = -kT\ln(EQE_{EL})$) is due to non-radiative recombination, where EQE_{EL} is electroluminescence quantum efficiency of the solar cell when charge carriers are injected into the device in dark[53]. Low non-radiative V_{OC} losses are made possible when the EQE_{EL} is enhanced. In other words, a great solar cell also needs to be a great light-emitting diode[54]. Generally, OSCs have much stronger non-radiative V_{OC} losses (in the range of 0.30–0.48 V) compared with highly efficient inorganic or perovskite solar cells[49,52]. From this analysis it becomes obvious that systems with small driving energies can still exhibit large voltage losses due to strong non-radiative recombination.

The origin of strong non-radiative recombination in OSCs has puzzled the community for almost a decade. A recent study shows that non-radiative recombination increased with decreasing CT energy of the blends[55]. The results were interpreted based on the 'energy-gap law' of non-radiative voltage losses, which were assigned to intramolecular vibrations of the organic semiconductor material itself. This model implied that non-radiative recombination is intrinsic to organic semiconductors that have high vibrational carbon–carbon frequency modes. However, while ref. 55 studied a large number of systems, the majority of these systems employed fullerene derivatives as the acceptor, with significant driving energy for charge transfer. The nature of the donor–fullerene π–π intermolecular interactions may limit the radiative emission rates for these materials systems, and it is not a priori clear whether the conclusions of ref. 55 generalize to non-fullerene OSCs, especially those with negligible driving energies.

A recent article investigated non-radiative recombination in non-fullerene OSCs with negligible driving energies[9]. The FTPS-EQE and EL spectrum of the blend device overlapped with those of the device based on the pristine donor material, indicating that the emission might be from singlet excitons, rather than CT states (Fig. 3a). In addition, the non-radiative recombination voltage loss of the optimized device approached that of the device based on the pristine donor material. These results imply that, in devices with negligible driving energies, the non-radiative recombination is possibly determined by the emission properties of the pristine material with the lowest bandgap. In other words, it means that in such devices it is important to enhance the photoluminescence quantum efficiency of the low-bandgap materials to decrease the non-radiative recombination loss. In an ideal case, no photoluminescence quenching of the low-bandgap material should be observed upon mixing the donor and acceptor at the V_{OC} so that the photovoltage can be maximized, while the photoluminescence should be completely quenched upon small internal field and at the J_{SC} so that the fill factor (FF) and photocurrent can be maximized. However, since only one combination was investigated in ref. 9, it is difficult to draw general conclusions, especially considering that the observation is purely experimental, without any mechanistic understanding. Further studies combining experimental and theoretical investigations, especially on systems with negligible driving energies, might shed more light on the origins of non-radiative recombination loss in OSCs. Since the voltage loss due to charge transfer is minimized in systems with negligible driving energies, a thorough understanding of non-radiative recombination is key to further enhancing the V_{OC} and hence the PCE of OSCs.

Spin statistics might be also important for understanding the nature of the non-radiative non-geminate recombination mechanisms. Following the very well understood issues of the spin statistics for electron–hole capture in organic light-emitting diodes (75% of these events form triplet excitons that are not emissive and often too low in energy to return to the emissive singlet state), the same spin statistics are expected for non-geminate recombination of electron–hole pairs in OSCs. Where there is a molecular triplet on either donor or acceptor that lies lower in energy than the CT

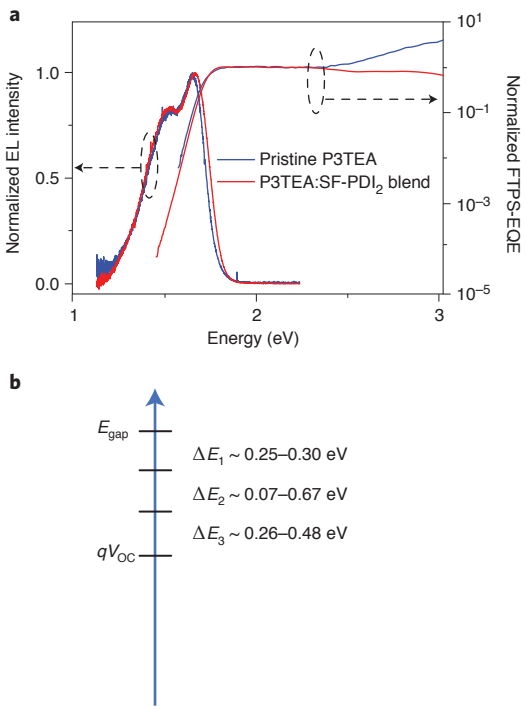

Figure 3 | Energy losses in NF OSCs. a, The FTPS-EQE and emission spectra of the blend overlap with those of the pristine devices when the driving energy between the donor and acceptor materials approaches zero. **b**, The energy losses from the E_{gap} to the qV_{OC}. The value ranges reported in literature are indicated in the figure. ΔE_1 is unavoidable for any solar cells and ΔE_2 was reported to be as small as 70 meV in the P3TEA:SF-PDI_2 blend, where the driving energy between the donor and acceptor materials approaches zero, leaving ΔE_3 critically important for further enhancing the V_{OC} of OSCs. Adapted from ref. 9, Macmillan Publishers Ltd (**a**).

energy gap, population of this state via the initially created triplet CT state causes very efficient non-radiative decay. This has been seen for a number of fullerene systems[56], though this is avoided under optimum circumstances, where the CT states formed are only weakly bound (as found for systems with well-formed pure fullerene nanostructures that probably confine the electron away from the fullerene cluster surface)[57]. At present, little is known about this triplet recombination channel for NF acceptor systems.

In addition to non-radiative recombination, another key point is the charge generation process in NF OSCs. Compared with the rapid development in materials and devices, photophysical investigations of the charge generation process are currently lagging behind, with few publications available in literature[9,58,59]. For fullerene-based OSCs, charge generation is a most intensively investigated issue[3,60–64]. Various studies found that the initial charge transfer process to form the CT excitation is ultrafast, on a timescale of tens of femtoseconds, suggesting that the charge separation process might involve delocalization of acceptor and donor states across the heterojunction[65–67]. The delocalization could be due to strong electronic coupling or vibronic (vibrational/electronic) coupling or entropy. Subsequent separation of the electron–hole pair to beyond the geminate recombination range, considered to be >5 nm (Langevin radius), has been measured to be very fast (as short as 40 fs)[3], and the presence of fullerene clusters that provide delocalized π^* electron wavefunctions over many fullerene units was often believed to play a key role for delocalisation or strong coupling[68]. After early time rapid separation, localization of the charge carrier wavefunction does set in, as the phonon cloud catches up with electrons[3,64,65]. It would be very interesting to investigate whether similar or different mechanisms are contributing to the charge separation process in NF OSCs, using advanced spectroscopic methods like broadband pump–probe spectroscopy, two-dimensional electronic spectroscopy[69,70], or pump–push–probe spectroscopy[71]. Based on the understanding developed for fullerene acceptors, a key requirement is the availability of charge carrier states (electron and/or holes) that are delocalized over many acceptor/donor molecules, so that long-range charge separation can occur before phonon-driven localization sets in.

Opportunities and challenges

The emergence of these NF acceptors provides a range of research directions to explore, which are otherwise not possible in fullerene-based OSCs. We now discuss these opportunities along with challenges from the viewpoints of materials and devices.

Material chemistry of photoactive materials. Enhancing both the photocurrent and photovoltage of NF OSCs by tuning independently the absorption spectra and the energetic levels, a key advantage for these devices, might be the most straightforward strategy to increase the photovoltaic efficiency (Fig. 2a,b). In fact, rapid progress in high-performance NF OSCs has been recently achieved by carefully tuning these two parameters. We use the device based on the PBDT-T-SF:IT-4F donor–acceptor system (Fig. 1f), with PCE = 13.1%, as an example to demonstrate possible approaches to further enhancing the efficiency. Although this blend shows a broad EQE spectrum with a maximum value of 83%, the EQE value at wavelengths ranging from 400 to 550 nm is still low due to limited absorption of the polymer donor in this region. In addition, the blend has a bandgap of 1.58 eV with a V_{OC} of 0.88 V, corresponding to a voltage loss of 0.70 eV, which can be also decreased further[9]. Therefore, additional improvement of the photocurrent of this system may be obtained by optimizing the absorption of the polymer donor in the short wavelength regime—for instance, by either shifting the polymer absorption spectrum to higher energies or by adding conjugated side chains to enhance the absorption of short wavelength regime. Photovoltage increase may be obtained by optimizing the energetic offsets between the donor and acceptor materials—for instance, by downshifting the energetic levels of the donor and/or upshifting those of the acceptor.

In addition to absorption spectra and energetic levels, morphology is also of critical importance to the device performance. State-of-the-art small molecules are all amorphous and also readily miscible with a range of high-performance polymer donors, raising new requirements for polymer donors to form optimized morphology. In this case, an effective approach to control phase separation would be to leverage the aggregation effects of the donor materials. Indeed, all the polymer donors in high-efficiency NF OSCs show strong aggregation tendency together with excellent dispersibility in a solvent[72–74]. The aggregation effects can be examined by temperature-dependent absorption measurements, as shown in Fig. 4a with PBDB-T as an example[75]. When mixed with small molecular acceptors, the aggregation of these donor polymers confines the nucleation and growth of the acceptors, forming phases with high purity and optimized morphology (Fig. 4b). The aggregation of the polymer donors can be tuned by changing the solvation of the molecules in solvent—for instance, by changing the solvent or by changing flexible side groups of the molecules. We believe that detailed investigations from the polymer physics point of view will help to further understand the process and provide practical guidance for rational design of materials.

Another critical morphology issue for NF OSCs is the molecular orientation at the D:A interfaces[18–21]. Charge transfer and transport in organic semiconductors occur preferentially in the vertical direction relative to their conjugated surfaces, through the sp^2 hybrid π-orbitals[76,77]. Therefore, the molecular orientation at these interfaces greatly affects the photovoltaic performance of OSCs. For instance, morphological studies of all-polymer OSCs found that face-to-face packing at the D:A interfaces was more favourable for charge generation than edge-to-face packing[18]. Although molecular orientation is not critical for OSCs based on fullerene derivatives, which have isotropic conjugated structures, it is a key parameter in NF OSCs due to the anisotropic shape of the conjugated backbone of NF acceptors. The precise characterization and control of molecular orientation will be important for the further development of these devices.

Charge carrier mobility can also significantly affect the device performance by affecting bimolecular recombination. For organic semiconductors, planar conjugated backbones and high crystallinity are beneficial for intra and inter molecular carrier transport, respectively. However, obtaining planar conjugated backbones and/or high crystallinity is not a simple task in BHJ OSCs, since a nanoscale interpenetrating network between D:A molecules is required for efficient charge generation. In order to meet this morphological requirement, high mobilities are sacrificed in state-of-the-art acceptor molecules. For example, as discussed previously, twisted backbones are employed in the small molecules based on PDI derivatives, and alkyls with high steric hindrance are employed in the ITIC-like molecules, limiting their electron transport capabilities. As a result, the electron mobilities of the active layers in high-efficiency NF OSCs could only reach 10^{-4} cm^2 s^{-1}, which is one or two orders of magnitude lower than that in fullerene-based OSCs. An important consequence is that the FF in NF OSCs always drops significantly when the active layer thickness increases from 100 nm to over 200 nm, mainly due to enhanced bimolecular recombination in thick films[6]. In contrast, fullerene-based OSCs can keep high FF with thicknesses up to a few hundreds of nanometers[7,78,79]. It is critically important to develop new molecular design strategies that can enhance the intermolecular π–π interactions without causing strong phase separation in blends. This will be very useful to enhance the EQE values by enhancing light absorption in thick films, and also important for making large area solar panels with

better reproducibility, which requires thickness tolerance during the solution-processed fabrication.

We have highlighted a few research directions to explore based on the parameters important for NF OSCs, including absorption spectra, energy levels, morphology (in terms on both aggregation and molecular orientation) and mobilities. We emphasize that the molecular design strategies to optimize one parameter might negatively affect another one, making it challenging to optimize all the parameters at the same time.

Devices. Tandem solar cells, where two or more sub-cells with complementary absorption bands are internally integrated, provide an effective approach to enhance the light absorption and reduce the thermal losses in single-junction solar cells[80–83]. The advantages of tandem structures have not been fully explored in fullerene-based OSCs, as they usually demonstrate large voltage losses. In contrast, NF OSCs can significantly enhance the PCE of tandem OSCs, thanks to their highly tunable absorption as well as the coexistence of low voltage losses and efficient charge separation. By carefully tuning the absorption of both front and rear sub-cells, NF-based tandem cells have demonstrated high PCEs of 13.8% (ref. 84) and more recently over 14% (ref. 85). A main reason for such a high efficiency is the reduced voltage loss. A critical challenge for current tandem NF OSCs is the photocurrent mismatch between the front and rear sub-cells. This can in principle be solved by increasing the thickness of both sub-cells with optimized bandgaps, so that different parts of the light spectrum can be effectivey absorbed by each sub-cell. However, as discussed previously, the efficiencies of thick NF OSCs are currently limited by poor charge transport.

In addition to tandem cells, ternary devices, where the active layer consists of three components, offer another feasible approach to extend the light absorption of the conventional binary OSCs[86,87]. The emergence of NF OSCs provides a wide range of possibilities for ternary devices: the third component can be a polymer or small molecule donor[88], a fullerene-based acceptor[89,90], or an NF acceptor (either polymer or small molecule)[91]. In addition to absorption and energy-level considerations, obtaining optimized morphology when a third component is added is critical to ternary devices. In cases where the third component is a fullerene derivative, the ratio of fullerene derivatives is usually kept low for good morphology. In order to significantly extend the light absorption, one of the effective approaches might be to use a third component that is similar to an existing component in chemical structure but different in absorption region. For example, a very recent work employed two ITIC-like acceptors (IT-M and IEICO) and demonstrated that these two acceptors are well miscible with each other[91]. With weight ratios changing from 1:0 to 0:1, the light absorbed by these two acceptors can always effectively contribute to the photocurrent generation. In addition, ternary devices have shown improved stability compared with binary devices[23]. Rich device physics might also be involved in these new ternary devices. For example, it was previously believed that the two donors or two acceptors in ternary devices form alloys, so that the V_{OC} lies between the V_{OC} values of two binary devices[89,92]. However, recently a ternary device demonstrated a V_{OC} value higher than the V_{OC} values of both binary devices[93]. This finding not only provides a unique approach to enhance the photovoltage of ternary devices, but also implies new device physics for ternary devices.

In some applications, absorbing only part of the light spectrum—rather than maximizing the light absorbed—could be useful. A typical example is semitransparent OSCs[94–96], which provide unique opportunities for niche applications—for instance, for smart windows. Ideal semitransparent OSCs are supposed to have weak absorption in the visible region and strong absorption in the near-infrared region[97]. In addition, a low voltage loss is also required for high efficiency. Fullerene-based OSCs can meet neither the

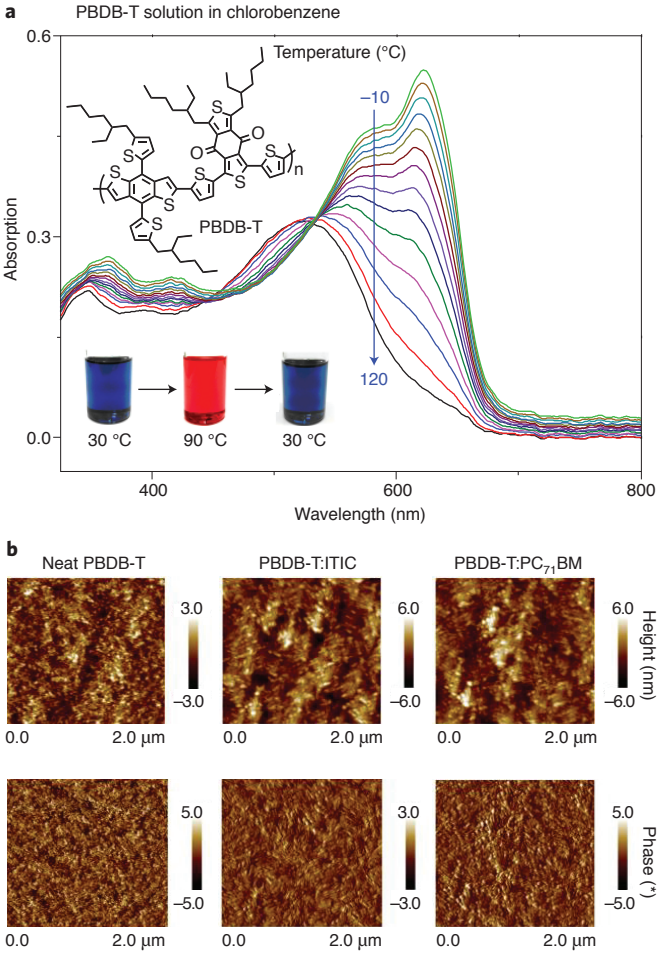

Figure 4 | The aggregation effects of the donor materials (PBDB-T as an example) in high-efficiency NF OSCs. a, Temperature-dependent absorption spectra of PBDB-T, which shows strong aggregation effects and good dispersibility in dilute solution. The inset shows that the solution is clear and that the temperature-dependent colour change is well reversible. **b**, The topography (top) and phase (bottom) images of the neat PBDB-T, PBDB-T:ITIC and PBDB-T:$PC_{71}BM$ films spin-coated from chlorobenzene solution under ambient temperature. The nanometre-sized aggregations can be clearly observed in the neat film, and the two blend films show very similar phase separation morphologies, indicating that the morphology of the blend films are mainly determined by the aggregation of the polymer.

absorption nor the small voltages loss requirements. Instead, NF OSCs provide the possibilities to meet both requirements. For example, a low-bandgap NF-acceptor (namely IEICO-4F) demonstrates great potential for this application[88]. Absorption of IEICO-4F mainly locates in the deep-red and near-infrared region, ranging from ~700 nm to ~1,000 nm. At the same time, it delivers a high V_{OC} (larger than 0.7 V), demonstrating a small voltage loss. In addition to the explorations of more NF acceptors for this application, efforts should also be devoted to achieving an optimized trade-off between transparency and conductivity of transparent electrodes.

Outlook

Previous efficiency predictions of OSCs are based on the assumption that significant driving energies are needed for efficient charge separation. Since NF OSCs have successfully demonstrated high quantum efficiency on negligible driving energies, we feel it necessary to re-estimate the efficiency (Fig. 5a). All the parameters can be empirically estimated other than non-radiative recombination losses, which the community has yet to understand, as discussed

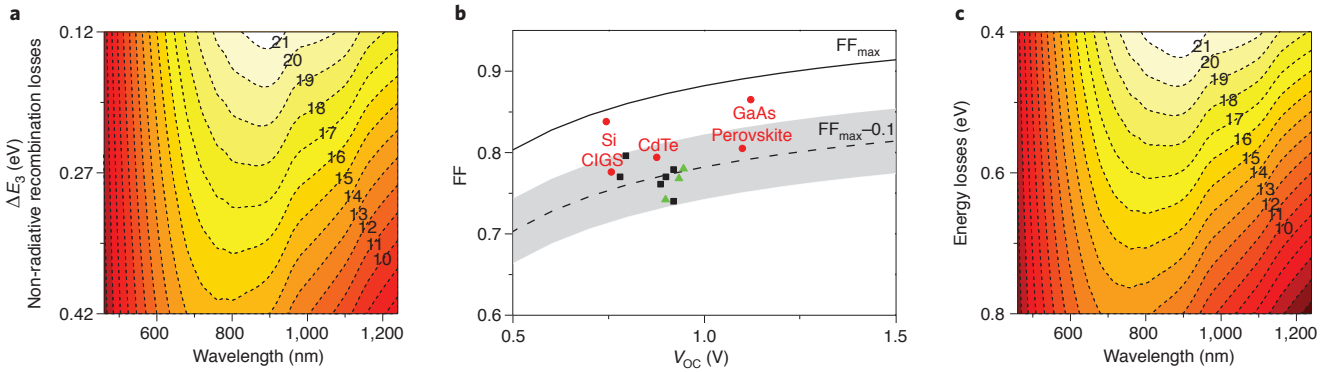

Figure 5 | New efficiency prediction for OSCs based on NF acceptors. a, Efficiency prediction (plotted in colour scale, with numbers on the contour lines representing PCE in %) for NF OSCs based on the assumption that they can work efficiently upon negligible driving energies. This figure highlights the importance of reducing the non-radiative recombination losses to further enhance the PCEs. **b**, Empirical relationship between the V_{OC} and the FF, together with the reported high-FF devices, including both inorganic and perovskite solar cells (in red), fullerene OSCs (in black), and NF OSCs (in green). The data are collected from refs 6,38,99–101. **c**, An alternative way to predict the efficiency of NF OSCs, showing the efficiency versus the energy losses.

previously. The EQE is assumed to be 85% above the bandgap; the V_{OC} is determined by equation (1), where ΔE_1 is calculated based on the bandgap, ΔE_2 is assumed to be 0.05 due to non-ideal band edge[9], and ΔE_3 (non-radiative recombination losses) is used as the y axis; the FF is based on the well-established empirical relationship[98]:

$$\mathrm{FF} = \frac{\gamma_{OC} - \ln(\gamma_{OC} + 0.72)}{\gamma_{OC} + 1} \quad (2)$$

where $\gamma_{OC} = qV_{OC}/nkT$, q is the elementary charge, n is the diode ideality factor, k is the Bolztmann constant and T is the temperature. Figure 5b shows the maximum FF (FF_{max}) as a function of the V_{OC}, indicating that smaller voltage losses (hence larger V_{OC}) also mean larger possible FF for a given material. In reality, the FF cannot reach the maximum value even for crystalline GaAs and Si solar cells[99]. We summarize high-FF OSCs (based on both fullerene and NF acceptors) available in literature in the figure[6,38,100,101]. We find that the values lie within a range of $FF_{max} - (0.1 \pm 0.04)$, and an FF of $FF_{max} - 0.1$ is used in the efficiency estimation.

As expected, non-radiative recombination V_{OC} losses play a key role in determining the efficiency of the OSCs. A high efficiency of 19% is within reach at wavelengths around 860 ± 60 nm, if the non-radiative recombination V_{OC} loss could be decreased to ~0.21 V. Therefore, understanding and decreasing the non-radiative recombination is key to further enhancing the PCEs of NF OSCs. The non-radiative recombination losses can potentially originate from the materials and energetic levels[9,55]. In addition to decreasing non-radiative recombination, optimizing the EQE is also important to reach high efficiency. Although a high EQE of 83% was reported in the literature for NF OSCs, such a high value only covers a small wavelength range[6]. Especially, most of the high-efficiency NF OSCs show low EQE values at short wavelengths due to limited absorption in this region. The light absorption at short wavelengths can be enhanced by tuning the absorption of D:A materials or by employing thick or ternary films.

We realize that the characterization of non-radiative recombination losses is not readily accessible by most research groups, especially those focusing on materials and device development. In order to make it easy for the materials and device groups to identify the potentials of their practical devices, we also estimate the PCE versus the energy losses, as shown Fig. 5c. All the assumptions in this figure are the same as those in Fig. 5a, except the V_{OC}, which is now determined by difference between the bandgap and the energy losses.

High efficiency prediction, unique features of NF acceptors, and rapid recent advances in this field, make NF OSCs promising as a practically relevant technology. In order to transfer from the lab-scale devices to large-scale modules using low-cost printing techniques, there are several additional issues to be taken care of. First, green solvents are required for processing. Currently, the lab-scale high-efficiency NF OSCs are mainly processed from toxic chlorinated solvents (for instance, chloroform or chlorobenzene). Fortunately, compared to fullerene derivatives, NF acceptors show excellent solubility in a larger range of solvents, offering more possibilities to select green solvents. For example, a NF OSC with over 11% PCE was recently reported by using a mixture of tetrahydrofuran and isopropanol as processing solvents, which are low toxic and also biodegradable[58]. Second, thickness tolerance is preferable for large-scale applications. Currently, the efficiency of NF OSCs drops significantly with increasing thickness from 100 to 250 nm, mainly due to decreasing FF[6]. As discussed previously, future efforts to increase the carrier mobilities might help to solve this problem. Third, detailed investigations on stabilities are needed[23]. It is well acknowledged that anisotropic NF acceptors with rigid backbones are less mobile than fullerenes in the blend, leading to better morphological stability than fullerene-based OSCs, which have been proved in a few highly efficient NF OSCs[22]. However, stability of NF OSCs under different environmental factors (for instance, oxygen, moisture and elevated temperatures) needs to be systematically studied. Fourth, new donor and acceptor materials need to be developed. State-of-the-art NF OSC donor and acceptor materials are based on complicated synthesis routes, making the cost of NF OSCs high. It will be desirable for future applications to design new materials, which combine low cost and high performance.

Received 27 September 2017; accepted 6 December 2017; published online 23 January 2018

References

1. Halls, J. J. M. *et al.* Efficient photodiodes from interpenetrating polymer networks. *Nature* **376,** 498–500 (1995).
2. Yu, G., Gao, J., Hummelen, J. C., Wudl, F. & Heeger, A. J. Polymer photovoltaic cells: enhanced efficiencies via a network of internal donor-acceptor heterojunctions. *Science* **270,** 1789–1791 (1995).
3. Gélinas, S. *et al.* Ultrafast long-range charge separation in organic semiconductor photovoltaic diodes. *Science* **343,** 512–516 (2014).
4. Schmidt-Mende, L. *et al.* Self-organized discotic liquid crystals for high-efficiency organic photovoltaics. *Science* **293,** 1119–1122 (2001).
5. McNeill, C. R. & Greenham, N. C. Conjugated-polymer blends for optoelectronics. *Adv. Mater.* **21,** 3840–3850 (2009).
6. Zhao, W. *et al.* Molecular optimization enables over 13% efficiency in organic solar cells. *J. Am. Chem. Soc.* **139,** 7148–7151 (2017).
7. Zhao, J. *et al.* Efficient organic solar cells processed from hydrocarbon solvents. *Nat. Energy* **1,** 15027 (2016).

8. Zhang, S., Ye, L. & Hou, J. Breaking the 10% efficiency barrier in organic photovoltaics: morphology and device optimization of well-known PBDTTT polymers. *Adv. Energy Mater.* **6,** 1502529 (2016).
9. Liu, J. *et al.* Fast charge separation in a non-fullerene organic solar cell with a small driving force. *Nat. Energy* **1,** 16089 (2016).
10. Cheng, P. *et al.* Realizing small energy loss of 0.55 eV, high open-circuit voltage >1 V and high efficiency >10% in fullerene-free polymer solar cells via energy driver. *Adv. Mater.* **29,** 1605216 (2017).
11. Chen, S. *et al.* A wide-bandgap donor polymer for highly efficient non-fullerene organic solar cells with a small voltage loss. *J. Am. Chem. Soc.* **139,** 6298–6301 (2017).
12. Baran, D. *et al.* Reduced voltage losses yield 10% efficient fullerene free organic solar cells with >1 V open circuit voltages. *Energy Environ. Sci.* **9,** 3783–3793 (2016).
13. Bin, H. *et al.* 11.4% Efficiency non-fullerene polymer solar cells with trialkylsilyl substituted 2D-conjugated polymer as donor. *Nat. Commun.* **7,** 13651 (2016).
14. Li, Y. *et al.* Non-fullerene acceptor with low energy loss and high external quantum efficiency: towards high performance polymer solar cells. *J. Mater. Chem. A* **4,** 5890–5897 (2016).
15. Vandewal, K. *et al.* Quantification of quantum efficiency and energy losses in low bandgap polymer:fullerene solar cells with high open-circuit voltage. *Adv. Funct. Mater.* **22,** 3480–3490 (2012).
16. Li, W., Hendriks, K. H., Furlan, A., Wienk, M. M. & Janssen, R. A. J. High quantum efficiencies in polymer solar cells at energy losses below 0.6 eV. *J. Am. Chem. Soc.* **137,** 2231–2234 (2015).
17. Ran, N. A. *et al.* Impact of interfacial molecular orientation on radiative recombination and charge generation efficiency. *Nat. Commun.* **8,** 79 (2017).
18. Ye, L. *et al.* Manipulating aggregation and molecular orientation in all-polymer photovoltaic cells. *Adv. Mater.* **27,** 6046–6054 (2015).
19. Jung, J. W. *et al.* Fluoro-substituted n-type conjugated polymers for additive-free all-polymer bulk heterojunction solar cells with high power conversion efficiency of 6.71%. *Adv. Mater.* **27,** 3310–3317 (2015).
20. Lee, J. *et al.* A nonfullerene small molecule acceptor with 3D interlocking geometry enabling efficient organic solar cells. *Adv. Mater.* **28,** 69–76 (2016).
21. Kang, H. *et al.* From fullerene–polymer to all-polymer solar cells: the importance of molecular packing, orientation, and morphology control. *Acc. Chem. Res.* **49,** 2424–2434 (2016).
22. Zhao, W. *et al.* Fullerene-free polymer solar cells with over 11% efficiency and excellent thermal stability. *Adv. Mater.* **28,** 4734–4739 (2016).
23. Baran, D. *et al.* Reducing the efficiency-stability-cost gap of organic photovoltaics with highly efficient and stable small molecule acceptor ternary solar cells. *Nat. Mater.* **16,** 363–369 (2017).
24. Cnops, K. *et al.* 8.4% efficient fullerene-free organic solar cells exploiting long-range exciton energy transfer. *Nat. Commun.* **5,** 3406 (2014).
25. Li, T. *et al.* Small molecule near-infrared boron dipyrromethene donors for organic tandem solar cells. *J. Am. Chem. Soc.* **139,** 13636–13639 (2017).
26. Tang, C. W. Two-layer organic photovoltaic cell. *Appl. Phys. Lett.* **48,** 183–185 (1986).
27. Anthony, J. E., Facchetti, A., Heeney, M., Marder, S. R. & Zhan, X. n-type organic semiconductors in organic electronics. *Adv. Mater.* **22,** 3876–3892 (2010).
28. Zhang, X. *et al.* A potential perylene diimide dimer-based acceptor material for highly efficient solution-processed non-fullerene organic solar cells with 4.03% efficiency. *Adv. Mater.* **25,** 5791–5797 (2013).
29. Lin, Y. *et al.* A twisted dimeric perylene diimide electron acceptor for efficient organic solar cells. *Adv. Energy Mater.* **4,** 1400420 (2014).
30. Nielsen, C. B., Holliday, S., Chen, H.-Y., Cryer, S. J. & McCulloch, I. Non-fullerene electron acceptors for use in organic solar cells. *Acc. Chem. Res.* **48,** 2803–2812 (2015).
31. Guo, Y. *et al.* Improved performance of all-polymer solar cells enabled by naphthodiperylenetetraimide-based polymer acceptor. *Adv. Mater.* **29,** 1700309 (2017).
32. Mori, D., Benten, H., Okada, I., Ohkita, H. & Ito, S. Highly efficient charge-carrier generation and collection in polymer/polymer blend solar cells with a power conversion efficiency of 5.7%. *Energy Environ. Sci.* **7,** 2939–2943 (2014).
33. Li, S. *et al.* Green-solvent-processed all-polymer solar cells containing a perylene diimide-based acceptor with an efficiency over 6.5%. *Adv. Energy Mater.* **6,** 1501991 (2016).
34. Gao, L. *et al.* All-polymer solar cells based on absorption-complementary polymer donor and acceptor with high power conversion efficiency of 8.27%. *Adv. Mater.* **28,** 1884–1890 (2016).
35. Fan, B. *et al.* Optimisation of processing solvent and molecular weight for the production of green-solvent-processed all-polymer solar cells with a power conversion efficiency over 9%. *Energy Environ. Sci.* **10,** 1243–1251 (2017).
36. Granström, M. *et al.* Laminated fabrication of polymeric photovoltaic diodes. *Nature* **395,** 257–260 (1998).
37. Lin, Y. *et al.* An electron acceptor challenging fullerenes for efficient polymer solar cells. *Adv. Mater.* **27,** 1170–1174 (2015).
38. Li, S. *et al.* Energy-level modulation of small-molecule electron acceptors to achieve over 12% efficiency in polymer solar cells. *Adv. Mater.* **28,** 9423–9429 (2016).
39. Yao, H. *et al.* Achieving highly efficient nonfullerene organic solar cells with improved intermolecular interaction and open-circuit voltage. *Adv. Mater.* **29,** 1700254 (2017).
40. Cha, H. *et al.* An efficient, 'burn in' free organic solar cell employing a nonfullerene electron acceptor. *Adv. Mater.* **29,** 1701156 (2017).
41. Faist, M. A. *et al.* Competition between the charge transfer state and the singlet states of donor or acceptor limiting the efficiency in polymer:fullerene solar cells. *J. Am. Chem. Soc.* **134,** 685–692 (2012).
42. Veldman, D., Meskers, S. C. J. & Janssen, R. A. J. The energy of charge-transfer states in electron donor–acceptor blends: insight into the energy losses in organic solar cells. *Adv. Funct. Mater.* **19,** 1939–1948 (2009).
43. Clarke, T. M. & Durrant, J. R. Charge photogeneration in organic solar cells. *Chem. Rev.* **110,** 6736–6767 (2010).
44. Kawashima, K., Tamai, Y., Ohkita, H., Osaka, I. & Takimiya, K. High-efficiency polymer solar cells with small photon energy loss. *Nat. Commun.* **6,** 10085 (2015).
45. Li, S. *et al.* A spirobifluorene and diketopyrrolopyrrole moieties based non-fullerene acceptor for efficient and thermally stable polymer solar cells with high open-circuit voltage. *Energy Environ. Sci.* **9,** 604–610 (2016).
46. Nikolis, V. C. *et al.* Reducing voltage losses in cascade organic solar cells while maintaining high external quantum efficiencies. *Adv. Energy Mater.* **7,** 1700855 (2017).
47. Rau, U., Blank, B., Müller, T. C. M. & Kirchartz, T. Efficiency potential of photovoltaic materials and devices unveiled by detailed-balance analysis. *Phys. Rev. Appl.* **7,** 044016 (2017).
48. Goris, L. *et al.* Absorption phenomena in organic thin films for solar cell applications investigated by photothermal deflection spectroscopy. *J. Mater. Sci.* **40,** 1413–1418 (2005).
49. Vandewal, K., Tvingstedt, K., Gadisa, A., Inganäs, O. & Manca, J. V. On the origin of the open-circuit voltage of polymer–fullerene solar cells. *Nat. Mater.* **8,** 904–909 (2009).
50. Tvingstedt, K. *et al.* Electroluminescence from charge transfer states in polymer solar cells. *J. Am. Chem. Soc.* **131,** 11819–11824 (2009).
51. Shockley, W. & Queisser, H. J. Detailed balance limit of efficiency of p-n junction solar cells. *J. Appl. Phys.* **32,** 510–519 (1961).
52. Yao, J. *et al.* Quantifying losses in open-circuit voltage in solution-processable solar cells. *Phys. Rev. Appl.* **4,** 014020 (2015).
53. Ross, R. T. Some Thermodynamics of photochemical systems. *J. Chem. Phys.* **46,** 4590–4593 (1967).
54. Miller, O. D., Yablonovitch, E. & Kurtz, S. R. Strong internal and external luminescence as solar cells approach the Shockley–Queisser limit. *IEEE J. Photovolt.* **2,** 303–311 (2012).
55. Benduhn, J. *et al.* Intrinsic non-radiative voltage losses in fullerene-based organic solar cells. *Nat. Energy* **2,** 17053 (2017).
56. Menke, S. M. *et al.* Limits for recombination in a low energy loss organic heterojunction. *ACS Nano* **10,** 10736–10744 (2016).
57. Rao, A. *et al.* The role of spin in the kinetic control of recombination in organic photovoltaics. *Nature* **500,** 435–439 (2013).
58. Zheng, Z. *et al.* Efficient charge transfer and fine-tuned energy level alignment in a thf-processed fullerene-free organic solar cell with 11.3% efficiency. *Adv. Mater.* **29,** 1604241 (2017).
59. Tamai, Y. *et al.* Ultrafast long-range charge separation in nonfullerene organic solar cells. *ACS Nano* https://doi.org/10.1021/acsnano.7b06575 (2017).
60. Vandewal, K. *et al.* Efficient charge generation by relaxed charge-transfer states at organic interfaces. *Nat. Mater.* **13,** 63–68 (2014).
61. Gao, F., Tress, W., Wang, J. & Inganäs, O. Temperature dependence of charge carrier generation in organic photovoltaics. *Phys. Rev. Lett.* **114,** 128701 (2015).
62. Deibel, C., Strobel, T. & Dyakonov, V. Role of the charge transfer state in organic donor–acceptor solar cells. *Adv. Mater.* **22,** 4097–4111 (2010).
63. Brédas, J.-L., Norton, J. E., Cornil, J. & Coropceanu, V. Molecular understanding of organic solar cells: the challenges. *Acc. Chem. Res.* **42,** 1691–1699 (2009).
64. Brédas, J.-L., Sargent, E. H. & Scholes, G. D. Photovoltaic concepts inspired by coherence effects in photosynthetic systems. *Nat. Mater.* **16,** 35–44 (2017).
65. Falke, S. M. *et al.* Coherent ultrafast charge transfer in an organic photovoltaic blend. *Science* **344,** 1001–1005 (2014).
66. Grancini, G. *et al.* Hot exciton dissociation in polymer solar cells. *Nat. Mater.* **12,** 29–33 (2013).
67. Jailaubekov, A. E. *et al.* Hot charge-transfer excitons set the time limit for charge separation at donor/acceptor interfaces in organic photovoltaics. *Nat. Mater.* **12,** 66–73 (2013).

68. Savoie, B. M. *et al.* Unequal partnership: asymmetric roles of polymeric donor and fullerene acceptor in generating free charge. *J. Am. Chem. Soc.* **136,** 2876–2884 (2014).
69. Song, Y., Clafton, S. N., Pensack, R. D., Kee, T. W. & Scholes, G. D. Vibrational coherence probes the mechanism of ultrafast electron transfer in polymer–fullerene blends. *Nat. Commun.* **5,** 4933 (2014).
70. Bakulin, A. A., Silva, C. & Vella, E. Ultrafast spectroscopy with photocurrent detection: watching excitonic optoelectronic systems at work. *J. Phys. Chem. Lett.* **7,** 250–258 (2016).
71. Bakulin, A. A. *et al.* The role of driving energy and delocalized states for charge separation in organic semiconductors. *Science* **335,** 1340–1344 (2012).
72. Liu, D. *et al.* Molecular design of a wide-band-gap conjugated polymer for efficient fullerene-free polymer solar cells. *Energy Environ. Sci.* **10,** 546–551 (2017).
73. Zhang, S. *et al.* A fluorinated polythiophene derivative with stabilized backbone conformation for highly efficient fullerene and non-fullerene polymer solar cells. *Macromolecules* **49,** 2993–3000 (2016).
74. Yao, H. *et al.* A wide bandgap polymer with strong π–π interaction for efficient fullerene-free polymer solar cells. *Adv. Energy Mater.* **6,** 1600742 (2016).
75. Qian, D. *et al.* Design, application, and morphology study of a new photovoltaic polymer with strong aggregation in solution state. *Macromolecules* **45,** 9611–9617 (2012).
76. Salleo, A. Charge transport in polymeric transistors. *Mater. Today* **10,** 38–45 (March, 2007).
77. Hutchison, G. R., Ratner, M. A. & Marks, T. J. Intermolecular charge transfer between heterocyclic oligomers. effects of heteroatom and molecular packing on hopping transport in organic semiconductors. *J. Am. Chem. Soc.* **127,** 16866–16881 (2005).
78. Chen, Z. *et al.* Low band-gap conjugated polymers with strong interchain aggregation and very high hole mobility towards highly efficient thick-film polymer solar cells. *Adv. Mater.* **26,** 2586–2591 (2014).
79. Zhou, H. *et al.* Development of fluorinated benzothiadiazole as a structural unit for a polymer solar cell of 7% efficiency. *Angew. Chem. Int. Ed.* **50,** 2995–2998 (2011).
80. Kim, J. Y. *et al.* Efficient tandem polymer solar cells fabricated by all-solution processing. *Science* **317,** 222–225 (2007).
81. You, J. *et al.* A polymer tandem solar cell with 10.6% power conversion efficiency. *Nat. Commun.* **4,** 1446 (2013).
82. Gilot, J., Wienk, M. M. & Janssen, R. A. J. Measuring the external quantum efficiency of two-terminal polymer tandem solar cells. *Adv. Funct. Mater.* **20,** 3904–3911 (2010).
83. Liu, W. *et al.* Nonfullerene tandem organic solar cells with high open-circuit voltage of 1.97 V. *Adv. Mater.* **28,** 9729–9734 (2016).
84. Cui, Y. *et al.* Fine-tuned photoactive and interconnection layers for achieving over 13% efficiency in a fullerene-free tandem organic solar cell. *J. Am. Chem. Soc.* **139,** 7302–7309 (2017).
85. Cui, Y., Yao, H., Yang, C., Zhang, S. & Hou, J. Organic solar cells with an efficiency approaching 15%. *Acta Polym. Sin.* https://doi.org/10.11777/j.issn1000-3304.2018.17297 (2017).
86. Zhang, G. *et al.* High-performance ternary organic solar cell enabled by a thick active layer containing a liquid crystalline small molecule donor. *J. Am. Chem. Soc.* **139,** 2387–2395 (2017).
87. Lu, L., Xu, T., Chen, W., Landry, E. S. & Yu, L. Ternary blend polymer solar cells with enhanced power conversion efficiency. *Nat. Photon.* **8,** 716–722 (2014).
88. Yao, H. *et al.* Design, synthesis, and photovoltaic characterization of a small molecular acceptor with an ultra-narrow band gap. *Angew. Chem. Int. Ed.* **56,** 3045–3049 (2017).
89. Lu, H. *et al.* Ternary-blend polymer solar cells combining fullerene and nonfullerene acceptors to synergistically boost the photovoltaic performance. *Adv. Mater.* **28,** 9559–9566 (2016).
90. Zhao, W., Li, S., Zhang, S., Liu, X. & Hou, J. Ternary polymer solar cells based on two acceptors and one donor for achieving 12.2% efficiency. *Adv. Mater.* **29,** 1604059 (2017).
91. Yu, R. *et al.* Two well-miscible acceptors work as one for efficient fullerene-free organic solar cells. *Adv. Mater.* **29,** 1700437 (2017).
92. Khlyabich, P. P., Burkhart, B. & Thompson, B. C. Compositional dependence of the open-circuit voltage in ternary blend bulk heterojunction solar cells based on two donor polymers. *J. Am. Chem. Soc.* **134,** 9074–9077 (2012).
93. Wang, C. *et al.* Ternary organic solar cells with enhanced open circuit voltage. *Nano Energy* **37,** 24–31 (2017).
94. Chen, C.-C. *et al.* High-performance semi-transparent polymer solar cells possessing tandem structures. *Energy Environ. Sci.* **6,** 2714–2720 (2013).
95. Xu, G. *et al.* High-performance colorful semitransparent polymer solar cells with ultrathin hybrid-metal electrodes and fine-tuned dielectric mirrors. *Adv. Funct. Mater.* **27,** 1605908 (2017).
96. Zhang, M., Guo, X., Ma, W., Ade, H. & Hou, J. A large-bandgap conjugated polymer for versatile photovoltaic applications with high performance. *Adv. Mater.* **27,** 4655–4660 (2015).
97. Wang, W. *et al.* Fused hexacyclic nonfullerene acceptor with strong near-infrared absorption for semitransparent organic solar cells with 9.77% efficiency. *Adv. Mater.* **29,** 1701308 (2017).
98. Green, M. A. Solar cell fill factors: general graph and empirical expressions. *Solid State Electron.* **24,** 788 (1981).
99. Green, M. A., Emery, K., Hishikawa, Y., Warta, W. & Dunlop, E. D. Solar cell efficiency tables (version 47). *Prog. Photovolt. Res. Appl.* **24,** 3–11 (2016).
100. Jao, M.-H., Liao, H.-C. & Su, W.-F. Achieving a high fill factor for organic solar cells. *J. Mater. Chem. A* **4,** 5784–5801 (2016).
101. Li, S. *et al.* Design of a new small-molecule electron acceptor enables efficient polymer solar cells with high fill factor. *Adv. Mater.* **29,** 1704051 (2017).

Acknowledgements

We thank Thomas Kirchartz for insightful discussions. The work was supported by the National Natural Science Foundation of China (grant nos 91633301, 91333204, 51673201, 21325419 and 51711530159), the Chinese Academy of Sciences (grant no. XDB12030200), the Swedish Research Council VR (grant nos 2017-00744 and 2016-06146), the Swedish Energy Agency Energimyndigheten (2016-010174), the Swedish Government Strategic Research Area in Materials Science on Functional Materials at Linköping University (faculty grant no. SFO-Mat-LiU #2009-00971), the Engineering and Physical Sciences Research Council in the UK, and the Knut and Alice Wallenberg foundation (KAW) through a Wallenberg Scholar grant to O.I.

Additional information

Reprints and permissions information is available online at www.nature.com/reprints. Correspondence and requests for materials should be addressed to J.H. or F.G.

Competing financial interests

The authors declare no competing financial interests.